AD-A138 601 X-RAY PHOTOELECTRON AND AUGER ELECRRON SPECTROSCOPIC STUDY OF THE CDTE SU..(U) MASSACHUSETTS INST OF TECH CAMBRIDGE DEPT OF CHEMISTRY A J RICCO ET AL. 07 FEB 84 1/1

UNCLASSIFIED TR-41 N00014-75-C-0880 F/G 7/4 NL

END
FILMED
DTIC

1.0
1.1
1.25 1.4 1.6
2.8 3.2 3.6 4.0 2.2 2.0 1.8

MICROCOPY RESOLUTION TEST CHART
NATIONAL BUREAU OF STANDARDS-1963-A

REPORT DOCUMENTATION PAGE

READ INSTRUCTIONS BEFORE COMPLETING FORM

1. REPORT NUMBER: ONR TR-41	2. GOVT ACCESSION NO.
3. RECIPIENT'S CATALOG NUMBER	
4. TITLE (and Subtitle): X-Ray Photoelectron and Auger Electron Spectroscopic Study of the CdTe Surface Resulting from Various Surface Pretreatments: Correlation of Photoelectrochemical and Capacitance-Potential Behavior with Surface Chemical Composition	5. TYPE OF REPORT & PERIOD COVERED: Interim Technical Report
	6. PERFORMING ORG. REPORT NUMBER
7. AUTHOR(s): Antonio J. Ricco, Henry S. White and Mark S. Wrighton	8. CONTRACT OR GRANT NUMBER(s): N00014-75-C-0880
9. PERFORMING ORGANIZATION NAME AND ADDRESS: Department of Chemistry, Rm. 6-335, Massachusetts Institute of Technology, Cambridge, Massachusetts 02139, U.S.A.	10. PROGRAM ELEMENT, PROJECT, TASK AREA & WORK UNIT NUMBERS: NR 051-579
11. CONTROLLING OFFICE NAME AND ADDRESS: Office of Naval Research, Department of the Navy, Arlington, Virginia 22217	12. REPORT DATE: February 7, 1984
	13. NUMBER OF PAGES: 20
14. MONITORING AGENCY NAME & ADDRESS (if different from Controlling Office)	15. SECURITY CLASS. (of this report): Unclassified
	15a. DECLASSIFICATION/DOWNGRADING SCHEDULE

AD A138601

16. DISTRIBUTION STATEMENT (of this Report)

Approved for public release; reproduction is permitted for any purpose o the United States Government; distribution unlimited.

DTIC

17. DISTRIBUTION STATEMENT (of the abstract entered in Block 20, if different from Report)

Distribution of this document is unlimited.

MAR 5 84

18. SUPPLEMENTARY NOTES

Prepared for publication in the Journal of Vacuum Science and Technology.

19. KEY WORDS (Continue on reverse side if necessary and identify by block number)

X-Ray, Auger, electron, spectroscopy, cadmium telluride, surfaces

DTIC FILE COPY

20. ABSTRACT (Continue on reverse side if necessary and identify by block number)

The surface chemistry and stoichiometry of p- and n-type CdTe photoelectrode treated with oxidizing and reducing etches have been characterized by X-ray photoelectron and Auger electron spectroscopies. The results of surface analysi have been correlated with the photoelectrochemical and capacitance-potential behavior of the photoelectrodes. "Oxidized" surfaces are covered by a thin Te°/TeO_2 layer (or a thicker Te° layer, if the etching procedure is slightly altered), resulting in Fermi level pinning: a constant photovoltage is found for a wide range of redox potentials and potential-independent space charge layer (o

capacitance obtains. "Reduced" surfaces closely resemble ion sputtered CdTe in chemical state and stoichiometry, resulting in more nearly "ideal" behavior: the semiconductor/electrolyte interface is rectifying in the dark; capacitance-potential behavior follows the Mott-Schottky equation near flat band conditions and photovoltage varies with redox potential, from 0 to ~0.7 for p-CdTe.

OFFICE OF NAVAL RESEARCH

CONTRACT N00014-75-C-0880

Task No. NR 051-579

TECHNICAL REPORT NO. 41

"X-RAY PHOTOELECTRON AND AUGER ELECTRON SPECTROSCOPIC STUDY OF THE CdTe SURFACE RESULTING FROM VARIOUS SURFACE PRETREATMENTS: CORRELATION OF PHOTOELECTROCHEMICAL AND CAPACITANCE-POTENTIAL BEHAVIOR WITH SURFACE CHEMICAL COMPOSITION"

by

Antonio J. Ricco, Henry S. White, and Mark S. Wrighton

Prepared for Publication

in

The Journal of Vacuum Science and Technology

Department of Chemistry
Massachusetts Institute of Technology
Cambridge, Massachusetts 02139

February 7, 1984

SS ThM06 (ACCEPTED FOR ORAL PRESENTATION)

X-Ray Photoelectron and Auger Electron Spectroscopic Study of the CdTe Surface Resulting from Various Surface Pretreatments: Correlation of Photoelectrochemical and Capacitance-Potential Behavior with Surface Chemical Composition

Antonio J. Ricco, Henry S. White and Mark S. Wrighton*

Department of Chemistry
Massachusetts Institute of Technology
Cambridge, Massachusetts 02139

Abstract:

The surface chemistry and stoichiometry of p- and n-type CdTe photoelectrodes treated with oxidizing and reducing etches have been characterized by X-ray photoelectron and Auger electron spectroscopies. The results of surface analysis have been correlated with the photoelectrochemical and capacitance-potential behavior of the photoelectrodes. "Oxidized" surfaces are covered by a thin Te^0/TeO_2 layer (or a thicker Te^0 layer, if the etching procedure is slightly altered), resulting in Fermi level pinning: a constant photovoltage is found for a wide range of redox potentials and potential-independent space charge layer capacitance obtains. "Reduced" surfaces closely resemble ion sputtered CdTe in chemical state and stoichiometry, resulting in more nearly "ideal" behavior: the semiconductor/electrolyte interface is rectifying in the dark; capacitance-potential behavior follows the Mott-Schottky equation near flat band conditions; and photovoltage varies with redox potential, from 0 to ~0.7 V for p-CdTe. approx.

Prepared for publication in the Journal of Vacuum Science and Technology as part of the Symposium Proceedings of the 30th National American Vacuum Society Symposium.

Introduction

Several recent reports have revealed a relationship between CdTe surface composition and the photovoltage (or barrier height) obtained from CdTe/metal and CdTe/electrolyte junctions.[1-5] Vacuum cleavage,[3-6] cleavage in air,[3-9] and polishing followed by chemical etching[1-3,7-21] are the three commonly used methods of crystal surface preparation. The two latter methods generally result in non-stoichiometric, oxidized surfaces[1,2,4,7-13] that are contaminated with Te° and/or TeO_2 prior to semiconductor/metal or electrolyte junction formation. An only recently explored exception to the general rule of oxidized CdTe surfaces is obtained by treating CdTe with a chemical reducing agent, such as dithionite,[1,2] $S_2O_4^{2-}$, or hydrazine, N_2H_4.[22] Oxidized surfaces exhibit interfacial electronic properties characteristic of Fermi level pinning:[23,24] barrier heights, ϕ_B, and photovoltages, E_V, are nearly independent of the work function, ϕ_m, of the contacting metal[14,15] or the redox potential, E_{redox}, of the electrolytic solution.[1,2] In contrast, ϕ_B's obtained from vacuum cleaved or reductively etched CdTe depend strongly on ϕ_m or E_{redox} and are regarded as more nearly ideal.[23,25]

In this work we detail experiments using XPS and Auger spectroscopy that give a more complete understanding of the relationship between surface composition and the characteristics of the semiconductor/electrolyte junction. We correlate surface composition and the potential dependence of the interfacial capacitance[2] of oxidatively and reductively etched p- and n-CdTe in contact with CH_3CN/electrolyte. Further, we correlate photovoltage vs. redox potential[1,2] with surface composition of n- and p-CdTe. Measurements made previously on $S_2O_4^{2-}$ reduced CdTe have now been extended to N_2H_4 reduced CdTe.

Experimental

Crystal Preparation and Etching Procedures. Single crystals of p- and n-CdTe (Cleveland Crystals, Cleveland, OH) were polished to a mirror finish with 0.3 μm alumina. Crystals were then cleaned for 1 min in boiling 5 M KOH. The dichromate oxidizing etch was a 30 s immersion in 4 g $K_2Cr_2O_7$/10 ml HNO_3/20 ml H_2O. The 15% HNO_3 etch lasted 30 min. Prior to the reducing etches, the crystal surface was etched in $HNO_3/Cr_2O_7^{2-}$. The dithionite etch was a 3 min immersion in boiling 0.6 M $Na_2S_2O_4$/2.5 M NaOH. The hydrazine etch was either 5 min in 30% N_2H_4, pH 14, at ~50°C or ~15 min in 95% N_2H_4 at 25°C. After thorough rinsing, crystals were stored in an evacuated tube until surface analysis.

Surface Spectroscopy and Photoelectrochemical Methods. XPS and AES data were recorded on PDP 11/04-controlled Physical Electronics (Perkin Elmer) Model 548 and Model 590 spectrometers, respectively. Full details of instrumentation, spectrometer calibration, and data manipulation are given elsewhere.[2,26,27] Samples were grounded to the spectrometer. A full description of the preparation of p- and n-CdTe electrodes and details of the electrochemical and capacitance-voltage measurement techniques are published elsewhere.[1,2]

Results and Discussion

1. X-Ray Photoelectron Spectroscopy. To identify the chemical state of the CdTe surface, precise core electron binding energies, ±<0.1 eV, were measured for the Cd 3d, Te 3d, and C 1s levels.

Samples examined included oxidized CdTe etched with either HNO_3/ $Cr_2O_7^{2-}$ or 15% HNO_3; reduced CdTe etched with either $OH^-/S_2O_4^{2-}$ or N_2H_4; and Ar ion sputtered CdTe. Because Cd and Te have similar atomic weights preferential sputtering effects are expected to be minimal;[28,29] this has been confirmed experimentally.[13] For a given surface treatment, no significant or systematic differences between the spectra of n- and p-type CdTe were observed. To identify surface impurities and determine overall stoichiometry, a low resolution survey scan was obtained for each sample. In the following discussion, only the $3d_{5/2}$ binding energies of the Cd and Te 3d doublets are cited because the spin-orbit splitting is independent of oxidiation state, see Table I.

a. Chemical State. Figure 1 and Table I summarize the XPS results for oxidized, reduced, and ion sputtered CdTe. There is little difference in the Cd 3d binding energies for the various surface treatments, consistent with the absence of significant changes in the Cd oxidation state.[8] In contrast, the Te 3d binding energies show large differences. Ion sputtered CdTe has a single Te $3d_{5/2}$ peak at 572.5 eV, characteristic of Te^{2-}. Dithionite or hydrazine reduced CdTe has a very similar Te 3d region, with the addition in some cases of a weak line at ~3.5 eV higher binding energy than the Te^{2-} peak. This high energy peak, with an average intensity only 4% of that of the Te^{2-} line, is a result of limited air oxidation of the CdTe surface, and the Te $3d_{5/2}$ binding energy, ~576 eV, is characteristic of TeO_2.[31] A few of the dithionite reduced CdTe surfaces showed slight asymmetry on the high binding energy side of the Te^{2-} peak, due to the presence of a small amount of Te°. Thus, both reducing etches yield XPS binding energies which closely resemble bulk (ion sputtered) CdTe.

The Te 3d spectra of oxidized CdTe are quite different from those of reduced and ion sputtered samples. The dichromate etch results in the spectrum shown in Figure 1. The high energy Te $3d_{5/2}$ line, at 576.2 eV, is due to TeO_2 formed during the oxidizing etch and/or air oxidation of the surface following the etch. Allowing the dichromate oxidized samples to sit in air for ~2 weeks noticeably enhances the TeO_2 signals. The lower energy Te $3d_{5/2}$ peak, at 573.0 eV, is midway between the binding energies measured for Te^{2-} and Te°. This peak is quite broad (FWHM ~1.8 eV) compared to the width of the 3d lines for sputtered CdTe (1.56 eV) and sputtered Te° (1.3 eV). Together, these data suggest that both Te° and Te^{2-} are present on the dichromate oxidized surface, with the Te° being part of a thin layer of oxidation products left by the etch and the Te^{2-} belonging to bulk CdTe. Auger data support this assignment of Te^{2-} and Te°, <u>vide infra</u>. CdTe oxidized in 15% HNO_3 yields yet a different Te 3d spectrum. There is only a single Te $3d_{5/2}$ peak, but the binding energy, 573.3 eV, is characteristic of Te°. In fact, there is no Cd signal visible at all for such samples which, according to Auger depth profile analysis, are covered by a fairly thick Te° layer.[12,33,34]

The two Te $3d_{5/2}$ lines found for air oxidized elemental Te, Table I, indicate the presence of both Te° and an overlayer of TeO_2. Sputtered elemental Te has only a single Te $3d_{5/2}$ line, giving the binding energy for Te° of 573.5 eV.

<u>b. Stoichiometry.</u> The Te:Cd ratio obtained from sputtered CdTe using integrated 3d peak areas and correcting for atomic

sensitivity factors[32] is 1.0 ± 0.1 (Table II) supporting the conclusion (vide supra) that preferential sputtering is not a problem. For dithionite or hydrazine reduced CdTe, the ratio is 1.0 ± 0.3, with the rather large standard deviation an indication that the surface is not always precisely stoichiometric. The overall Te:Cd ratio of 1.6 for dichromate oxidized CdTe indicates a substantial enrichment of the surface in Te relative to the bulk, consistent with the hypothesis that the dichromate etch leaves oxidiation products of Te on the surface. This Te:Cd ratio, though greater than unity, is far less than that obtained by other workers using the same etch.[1,11] They found that the dichromate etch left a contaminant layer so thick that the Cd signal was entirely obscured. A possible explanation for this behavior is presented in the next section.

2. Auger Spectroscopy and Depth Profile Analysis. AES gives results for oxidized and reduced samples which are in qualitative agreement with the results from XPS. Figure 2a shows the Auger spectrum of dichromate oxidized CdTe. The Te/Cd ratios determined from AES for oxidized samples are significantly larger than those found by XPS (Table II), consistent with the difference in electron escape depths. For the Cd MNN Auger line, the kinetic energy (KE) of electrons is ~380 eV, giving an escape depth[33] of ~7Å; the Cd $3d_{5/2}$ line, excited by Mg Kα irradiation, gives electrons with KE ~850 eV, for an escape depth of ~15 Å. Thus, Auger data substantiate the hypothesis of bulk CdTe covered by a thin (<30Å) Te°/TeO_2 layer. A depth profile of dichromate etched CdTe, Figure 2b, shows that O extends nearly into the bulk, though the relative amount of O decreases with sputtering time, suggesting the

Te°/TeO_2 layer observed by XPS becomes richer in Te° as bulk CdTe is approached. This profile also shows that the surface contaminant layer is relatively thin. The Cd and Te signals reach their bulk values in <1 min at a sputtering current density of ~25 $\mu A/cm^2$ at 2 kV.

If a short time, ~30 s, elapses between the $Cr_2O_7^{2-}/HNO_3$ etch and the H_2O rinse, the CdTe surface becomes covered with Te°, Figure 2a. An Auger depth profile of such a sample, Figure 2c, reveals that little O is present in this layer and that it is fairly thick relative to the Te°/TeO_2 layer formed on "immediately rinsed" dichromate etched CdTe, Figure 2b. Presumably, this is the explanation for the difference in thickness of the Te°/TeO_2 layer found in the present study compared to that found by others.[1,11] The 15% HNO_3 etch gives a thick, dull-looking Te° layer, even if the crystal is rinsed immediately after etching.

With the exception of S and C impurity peaks, the Auger spectrum of dithionite reduced CdTe closely resembles that of Ar ion sputtered CdTe, Figure 2a. The S peak is presumably a result of impurities left behind by the dithionite etch. The sulfur does not, however, play an important role in the interfacial energetics of the reduced CdTe surfaces; an oxidized CdTe electrode may be electrochemically reduced to give the same differential capacitance vs. potential curve as obtained for a sample reduced with the dithionite etch. In addition, Auger spectroscopy reveals that N_2H_4 reduction of CdTe yields a nearly sulfur-free surface closely resembling that of ion sputtered CdTe. Importantly, the photoelectrochemical and capacitance-voltage behavior of hydrazine reduced p- and n-CdTe is quite similar to that obtained as a result of dithionite reduction.

3. Photoelectrochemical and Capacitance-Voltage Measurements.

Scheme I summarizes the situation for oxidatively etched p- and n-CdTe. Oxidized n-CdTe yields photovoltages of 500-600 mV for redox potentials between +0.7 and -1.7 V vs. SCE, while p-CdTe yields little or no photovoltage (E_V < 100 mV) for E_{redox} between

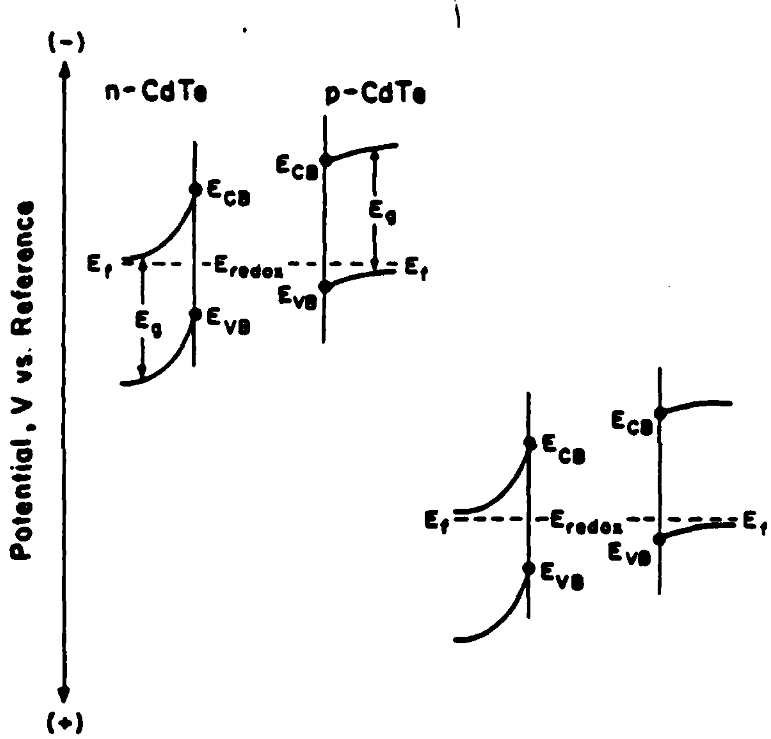

Scheme I. Interfacial energetics for oxidatively etched p- and n-CdTe for a range of solution redox potentials.[1,2] Potential drop across the Helmholtz double layer (not shown) accounts for the apparent shift in location of the valence and conduction bands, relative to an external reference potential, as the redox potential is varied.

+0.2 and -1.7 V vs. SCE. This suggests that the Fermi level of n-CdTe is pinned to a value at least ~0.6 V below the conduction band. For oxidized p-CdTe, the Fermi level is apparently pinned quite near the valence band edge. Capacitance-voltage measurements in CH_3CN/electrolyte (no redox couple) for oxidized CdTe reveal nearly potential-independent space charge layer capacitance

(~130 nF/cm^2 for n-type; ~50 nF/cm^2 for p-type), implying that the band bending is potential-independent and thus supporting the case made above for Fermi level pinning.[2]

When CdTe is reductively etched, either with dithionite or hydrazine, the interfacial energetics represented by Scheme II apply. In the case of n-CdTe, when E_{redox} is negative of -1.2 V vs. SCE, the approximate location of the conduction band edge, ohmic contact occurs between solution species and the semiconductor. But for E_{redox} between -1.1 and +0.1 V vs. SCE, an approximately linear relationship between E_V and E_{redox} holds, with $\Delta E_V/\Delta E_{redox} \cong 0.6$. For reduced p-CdTe, ohmic contact exists for redox potentials positive of the valence band edge, ~0.2 V vs. SCE, while E_V varies from 0 to ~0.65 V for E_{redox} between -0.3 and -1.8 V vs. SCE, with a maximum rate of change, $\Delta E_V/\Delta E_{redox}$, of 0.6. Capacitance-voltage measurements also suggest a more ideal interface for reduced CdTe, and linear Mott-Schottky plots are obtained. From the Mott-Schottky plots, values of the flat band potential and the donor (n-type, 2 x 10^{17} cm^{-3}) and acceptor (p-type, 2.5 x 10^{15} cm^{-3}) densities are calculated. The E_{FB} values and donor/acceptor densities allow calculation of the location of the valence and conduction band edges, yielding values of ~-0.2 and -1.5 V vs. SCE, respectively.

Conclusions

Surface spectroscopy reveals that the Fermi level pinned behavior characteristic of oxidized p- and n-CdTe is a result of oxidation products left on the surface after etching. Specifically, Te°, a small band gap semiconductor, E_g = 0.35 eV,[33,36] is found on the surface of oxidized samples. The Te°

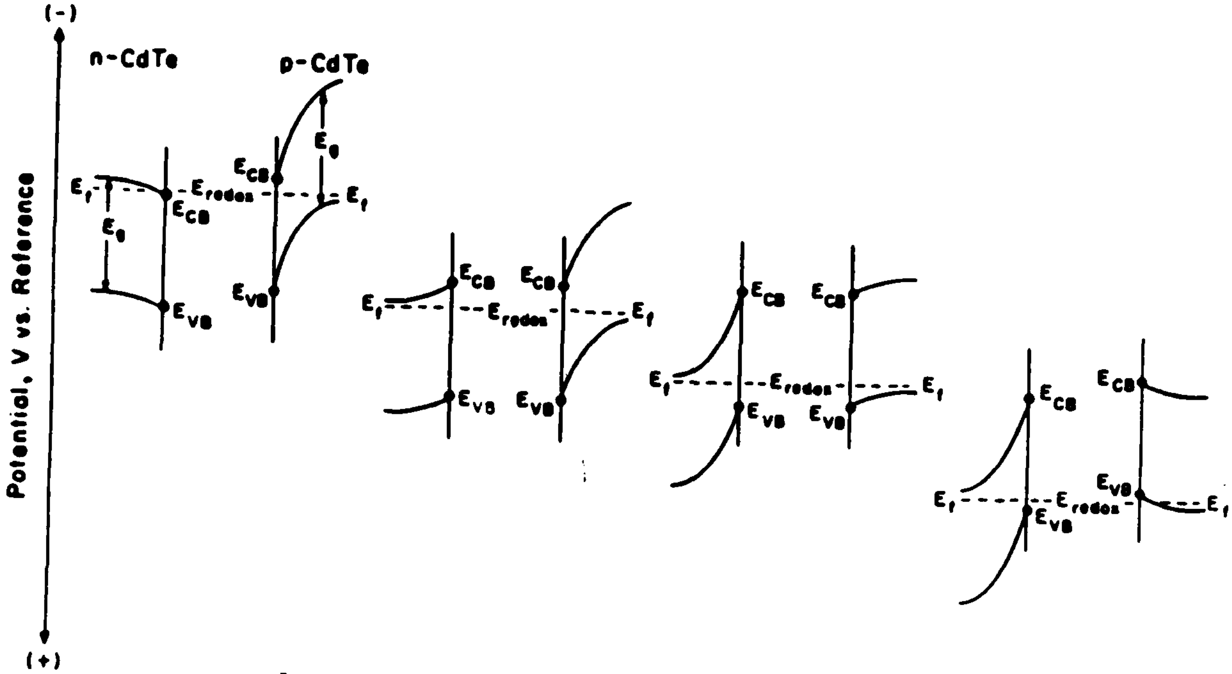

Scheme II. Interfacial energetics for reductively etched, stoichiometric *p*- and *n*-CdTe.[2] Note that the extent of band bending (and thus the barrier height and photovoltage) changes with redox potential. For very positive redox potentials at n-CdTe or very negative redox potentials at p-CdTe, the amount of band bending reaches its maximum, hence additional potential drop is across the Helmholtz layer, cf. Scheme I.

overlayer has a large work function[23] and would be expected to give a larger barrier on n- than on p-CdTe. This is entirely consistent with the reasonably large photovoltage obtained for surface oxidized n-CdTe and the near-zero photovoltage obtained for surface-oxidized p-CdTe in electrolyte/redox couple solutions. That Fermi level pinning is a result of the surface treatment is illustrated by the results from the reducing etches, namely the nearly ideal behavior of reduced p- and n-CdTe coupled with the close resemblance of the surface composition to clean CdTe. Because most solid state measurements have been made on air cleaved or oxidatively etched CdTe crystals, it is reasonable to conclude that the nearly constant barrier heights found in these studies result from the oxidation of the CdTe surface. Results from metal deposition on vacuum cleaved CdTe and from electrochemical studies on reduced CdTe support this conclusion.

Acknowledgements. This research was supported in part by the Office of Naval Research and in part by the National Science Foundation Materials Research Laboratory Program at the M.I.T. Center for Materials Science and Engineering.

References

1. S. Tanaka, J.A. Bruce, and M.S. Wrighton, J. Phys. Chem., 85, 3778 (1981).
2. H.S. White, A.J. Ricco, and M.S. Wrighton, J. Phys. Chem., in press.
3. T. Takebe, J. Saraie, and T. Tanaka, Phys. Status Solidi A, 47, 123 (1978).
4. (a) R.R. Varma, M.H. Patterson, and R.H. Williams, J. Phys. D: Appl. Phys., 12, L71 (1979); (b) T.P. Humphreys, M.H. Patterson, and R.H. Williams, J. Vac. Sci. Technol., 17, 886 (1980).
5. R.H. Williams and M.H. Patterson, Appl. Phys. Lett., 40, 484 (1982).
6. T.F. Huech, J. Appl. Phys., 52, 4874 (1981).
7. M.H. Patterson and R.H. Williams, J. Phys. D: Appl. Phys., 11, L83 (1978).
8. A. Ebina, K. Asario, and T. Takahashi, Phys. Rev. B, 22, 1980 (1980).
9. M. Hage-Ali, R. Stuck, A. N. Saxena, and P. Siffert, Appl. Phys., 19, 25 (1979).
10. J.P. Ponpon, Appl. Phys. A, 27, 11 (1982).
11. P. Gaugash and A.G. Milnes, J. Electrochem. Soc., 128, 924 (1981).
12. H.C. Montgomery, Solid State Electron., 7, 147 (1964).
13. U. Solzbach and H.J. Richter, Surf. Sci., 97, 191 (1980).
14. J.P. Ponpon, M. Saraphy, E. Buttung, and P. Siffert, Phys. Status Solidi A, 59, 259 (1980).
15. J.P. Ponpon, and P. Siffert, Rev. Phys. Appl., 12, 427 (1977).
16. B. Rabin, H. Tabatabai, and P. Siffert, Phys. Status Solidi A, 49, 577 (1978).
17. L. Nadjo, J. Electroanal. Chem., 108, 29, (1980).
18. A. Aruchamy and M.S. Wrighton, J. Phys. Chem., 84, 2848 (1980).
19. J. Touskova and R. Kuzel, Phys. Status Solidi A, 36, 747 (1976).
20. J.M. Pawlokowski and J. Zylinski, Acta Phys. Pol. A, A54, 155 (1978).
21. I. Gabas and J. Tousek, Phys. Status Solidi A, 43, 351 (1977).

22. (a) G.F. Fulop, T.F. Betz, P.V. Meyers, and M.E. Doty, U.S. Patent 4260427, April 7, 1980; U.S. Patent 4261802 April 14, 1981; (b) G. Fulop, M. Doty, P. Meyers, J. Betz, and C.H. Liu, Appl. Phys. Lett, 40, 327 (1982).
23. S.M. Sze, "Physics of Semiconductor Devices", 2nd ed., John Wiley & Sons: New York (1981).
24. A.J. Bard, A.B. Bocarsly, F.-R. F. Fan, E.G. Walton, and M.S. Wrighton, J. Am. Chem. Soc., 102, 3671 (1980).
25. H. Gerischer in "Physical Chemistry: An Advanced Treatise", H. Eyring, D. Henderson, and W. Jost, eds., Vol. 9A, Academic Press: New York (1970).
26. The software for computer control of the XPS spectrometer, as well as data acquisition and curve fitting, is part of the MACS (Version VI) software package: Physical Electronics Division, Perkin-Elmer Corp., Eden Prairie, MN.
27. C.D. Wagner, "Energy Calibration of Electron Spectrometers", Applied Surface Analysis, ASTM STP 699, T.L. Barr and L.E. Davis, eds., American Society for Testing and Materials, pp. 137-147 (1980).
28. M. Szymonski and R.S. Bhattacharya, Appl. Phys., 20, 207 (1979).
29. (a) H.H. Andersen, "Sputtering of Multicomponent Metals and Semiconductors", in SPIG 1980, B. Cobic, ed., Boris Kidric Institute of Nuclear Sciences, Beograd, Yugoslavia; (B) E. Zinner, J. Electrochem. Soc., 130, 199C (1983).
30. J.C. Phillips, "Bonds and Bands in Semiconductors", Academic Press: New York, Chapter 2, (1973).
31. M.K. Bahl, R.L. Watson, and K.J. Irgolic, J. Chem. Phys., 66, 5526 (1977).
32. C.D. Wagner, L.E. Davis, M.V. Zeller, J.A. Taylor, R.H. Raymond and L.H. Gale, Surf. and Interface Anal., 3, 211 (1981).
33. R.N. Zitter and D.L. Charda, J. Appl. Phys., 46, 1405 (1975).
34. R.N. Zitter, Surf. Sci., 28, 339 (1971).
35. C.J. Powell, Surf. Sci., 44, 29 (1974).
36. N.W. Ashcroft and N.D. Mermin, "Solid State Physics", Holt, Rinehart, and Winston: New York, p. 566 (1976).

Figure Captions

Figure 1. X-ray photoelectron spectra of the Te 3d region showing, from top: Ar ion sputtered CdTe; $S_2O_4^{2-}/OH^-$ reduced CdTe; N_2H_4 reduced CdTe; $Cr_2O_7^{2-}/HNO_3$ oxidized CdTe; and 15% HNO_3 oxidized CdTe.

Figure 2. (a) Auger spectra of CdTe showing, from top: $Cr_2O_7^{2-}/HNO_3$ oxidized CdTe, rinsed immediately after etching; $Cr_2O_7^{2-}/HNO_3$ oxidized CdTe, rinsed 30 s after etching; $S_2O_4^{2-}/OH^-$ reduced CdTe; and Ar ion sputtered CdTe. (b) Auger depth profile of $Cr_2O_7^{2-}/HNO_3$ oxidized CdTe, rinsed immediately after etching. (c) Auger depth profile of $Cr_2O_7^{2-}/HNO_3$ oxidized CdTe, rinsed 30 s after etching. The Ar ion current densities are the same for (b) and (c).

Table I.[a] Summary of XPS Multiplex[b] Data for Chemical State of Oxidized, Reduced, and Ion Sputtered CdTe.

Sample	Te $3d_{5/2}$ Core Level					Cd $3d_{5/2}$ Core Level			
	Assignment	Center[c]	$\Delta E_{3/2-5/2}$[d]	FWHM[e]	Intensity[f]	Center	$\Delta E_{3/2-5/2}$	FWHM	Intensity
Ion Sputtered CdTe	$^{2-}$	572.47(5)	10.40(1)	1.56(3)	1.1(1)	405.08(6)	6.76(0)	1.28(1)	1.0
$S_2O_4^{2-}$/NaOH Reduced CdTe	e^{2-}	572.50(7)	10.42(1)	1.79(12)	1.0(3)	404.94(7)	6.76(1)	1.27(6)	1.0
	TeO_2	575.96(11)	10.31(8)	1.57(4)	0.04(5)				
N_2H_4 Reduced CdTe	Te^{2-}	572.54(5)	10.41(4)	1.59(13)	1.0(3)	405.01(10)	6.76(1)	1.24(7)	1.0
	TeO_2	576.0(2)	10.4(2)	1.76(2)	0.04(8)				
$Cr_2O_7^{2-}/HNO_3$ Oxidized CdTe	"Mixed" Te^{2-}/Te°	572.98(11)	10.42(3)	1.83(6)	1.2(1)	405.15(7)	6.75(1)	1.37(5)	1.0
	TeO_2	576.21(10)	10.37(3)	1.68(12)	0.4(2)				
15% HNO_3 Oxidized CdTe	Te°	573.24(10)	10.37(3)	1.31(8)	1.0		None present		
Oxidized Elemental Te	Te°	573.5(10)	10.3(1)	1.2(2)	0.05(3)				
	TeO_2	576.4(2)	10.4(1)	1.6(2)	1.0				
Ion Sputtered Elemental Te	Te°	573.54(10)	10.38(3)	1.34(8)	1.0				

[a]Each tabulated value for CdTe is the average of 4–6 runs. Uncertainty in the last digit of each entry, given parenthetically, is estimated as twice the standard deviation of the average.
[b]Data obtained at 25 eV pass energy, 0.2 eV/point.
[c]Center of the $3d_{5/2}$ line from curve fit data, in eV.
[d]Separation of the $3d_{3/2}$ and $3d_{5/2}$ lines, in eV.
[e]Average full width at half-max minimum of the $3d_{3/2}$ and $3d_{5/2}$ lines, in eV.
[f]Relative intensities are calculated from integrated peak areas of the curve fit data and are corrected for atomic sensitivity factors as given in ref. 32.

Table II. Comparison of Stoichiometry Determined by XPS and AES for Reduced, Oxidized, and Ion Sputtered CdTe.

Sample	Relative Intensity[a,b]			
	Cd	Te		O
	XPS, AES	XPS	AES	XPS
Ion Sputtered CdTe	1.0	1.0(1)	1.0	0.0
$NaOH/S_2O^{2-}$ Reduced CdTe	1.0	1.0(2)	0.8(3)	1.5(7)
N_2H_4 Reduced CdTe	1.0	1.0(3)	1.1(2)	3.5(4)
$HNO_3/Cr_2O_7^{2-}$ Oxidized CdTe	1.0	1.6(3)	3.5(6)	4.0(6)
15% HNO_3 Oxidized CdTe	0.0	1.0	1.0	1.4(4)
Oxidized Elemental Te	---	1.0	---	1.9(5)

[a]Intensity for XPS data is taken from survey scans, 100 eV pass energy, by integrating the Cd $3d_{5/2}$, Te $3d_{5/2}$, and O 1s lines and correcting for the respective sensitivity factors.[32] The XPS intensities include all oxidiation states of each element, i.e. Te^{2-}, Te°, and TeO_2 are all included in the Te intensity.

[b]For AES data, relative intensity of Te to Cd was determined experimentally for ion sputtered CdTe using the MNN Auger lines. (Preferential sputtering effects are unimportant, see ref. 8 and text).

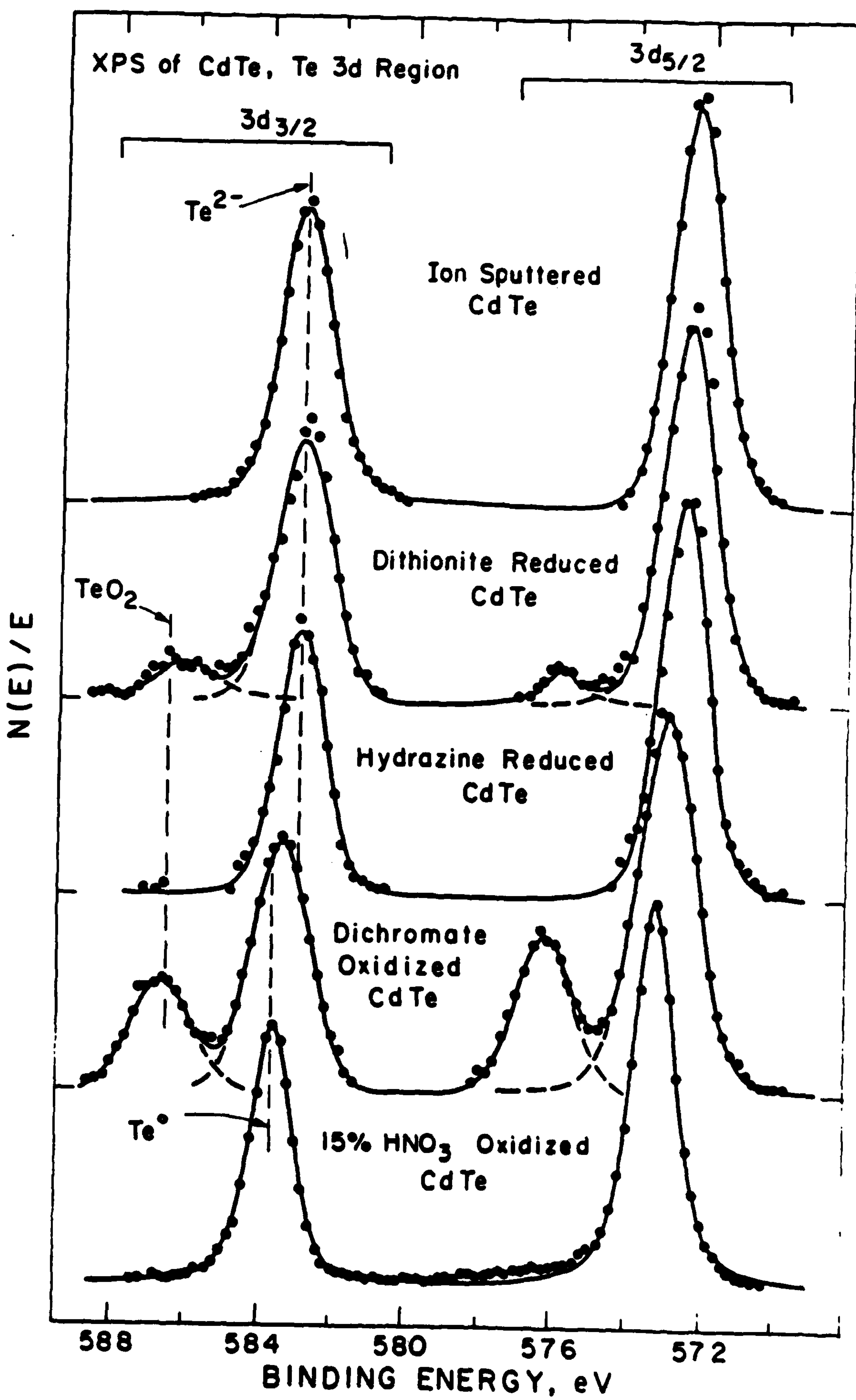

XPS of CdTe, Te 3d Region
$3d_{5/2}$
$3d_{3/2}$
Te^{2-}
Ion Sputtered CdTe
Dithionite Reduced CdTe
TeO_2
Hydrazine Reduced CdTe
Dichromate Oxidized CdTe
Te^{0}
15% HNO_3 Oxidized CdTe
N(E)/E
588
584
580
576
572
BINDING ENERGY, eV

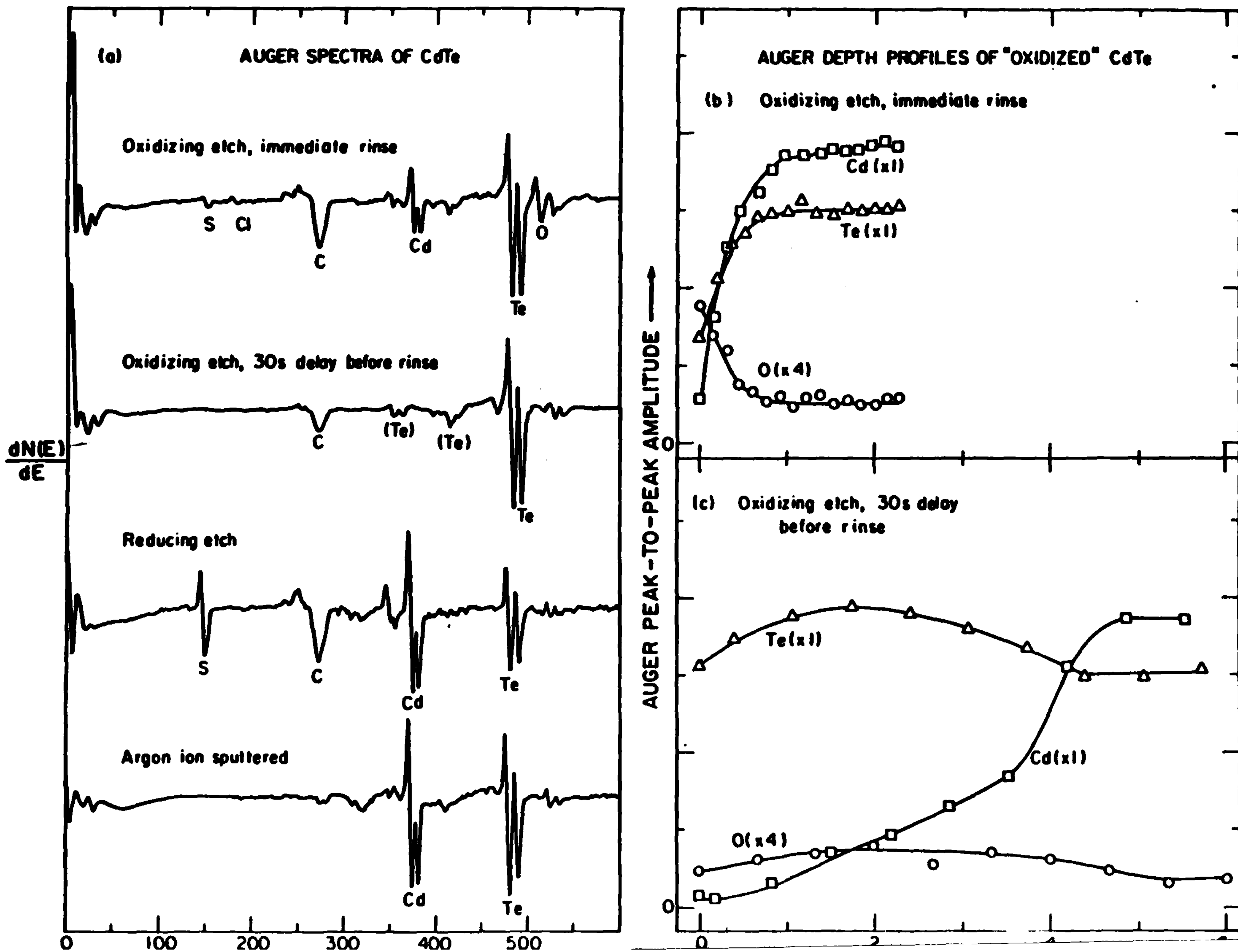
(a)
AUGER SPECTRA OF CdTe
Oxidizing etch, immediate rinse
S
Cl
C
Cd
Te
O
Oxidizing etch, 30s delay before rinse
C
(Te)
(Te)
Te
Reducing etch
S
C
Cd
Te
Argon ion sputtered
Cd
Te
dN(E)/dE
0
100
200
300
400
500
AUGER DEPTH PROFILES OF "OXIDIZED" CdTe
(b) Oxidizing etch, immediate rinse
Cd (x1)
Te (x1)
O (x4)
(c) Oxidizing etch, 30s delay before rinse
Te (x1)
Cd (x1)
O (x4)
AUGER PEAK-TO-PEAK AMPLITUDE
0
2

TECHNICAL REPORT DISTRIBUTION LIST, GEN

	No. Copies
Office of Naval Research Attn: Code 413 800 N. Quincy Street Arlington, Virginia 22217	2
ONR Pasadena Detachment Attn: Dr. R. J. Marcus 1030 East Green Street Pasadena, California 91106	1
Commander, Naval Air Systems Command Attn: Code 310C (H. Rosenwasser) Washington, D.C. 20360	1
Naval Civil Engineering Laboratory Attn: Dr. R. W. Drisko Port Hueneme, California 93401	1
Superintendent Chemistry Division, Code 6100 Naval Research Laboratory Washington, D.C. 20375	1
Defense Technical Information Center Building 5, Cameron Station Alexandria, Virginia 22314	12
DTNSRDC Attn: Dr. G. Bosmajian Applied Chemistry Division Annapolis, Maryland 21401	1
Naval Ocean Systems Center Attn: Dr. S. Yamamoto Marine Sciences Division San Diego, California 91232	1

	No. Copies
Naval Ocean Systems Center Attn: Technical Library San Diego, California 92152	1
Naval Weapons Center Attn: Dr. A. B. Amster Chemistry Division China Lake, California 93555	1
Scientific Advisor Commandant of the Marine Corps Code RD-1 Washington, D.C. 20380	1
Dean William Tolles Naval Postgraduate School Monterey, California 93940	1
U.S. Army Research Office Attn: CRD-AA-IP P.O. Box 12211 Research Triangle Park, NC 27709	1
Mr. Vincent Schaper DTNSRDC Code 2830 Annapolis, Maryland 21402	1
Mr. John Boyle Materials Branch Naval Ship Engineering Center Philadelphia, Pennsylvania 19112	1
Mr. A. M. Anzalone Administrative Librarian PLASTEC/ARRADCOM Bldg 3401 Dover, New Jersey 07801	1

TECHNICAL REPORT DISTRIBUTION LIST, 051A

Dr. M. A. El-Sayed
Department of Chemistry
University of California
Los Angeles, California 90024

Dr. E. R. Bernstein
Department of Chemistry
Colorado State University
Fort Collins, Colorado 80521

Dr. J. R. MacDonald
Chemistry Division
Naval Research Laboratory
Code 6110
Washington, D.C. 20375

Dr. G. B. Schuster
Chemistry Department
University of Illinois
Urbana, Illinois 61801

Dr. A. Adamson
Department of Chemistry
University of Southern California
Los Angeles, California 90007

Dr. M. S. Wrighton
Department of Chemistry
Massachusetts Institute of Technology
Cambridge, Massachusetts 02139

Dr. A. Paul Schaap
Department of Chemistry
Wayne State University
Detroit, Michigan 49207

Dr. Gary Bjorklund
IBM
5600 Cottle Road
San Jose, California 95143

Dr. Kent R. Wilson
Chemistry Department
University of California
La Jolla, California 92093

Dr. G. A. Crosby
Chemistry Department
Washington State University
Pullman, Washington 99164

Dr. R. Hautala
Chemical Research Division
American Cyanamid Company
Bound Brook, New Jersey 08805

Dr. J. I. Zink
Department of Chemistry
University of California
Los Angeles, California 90024

Dr. D. M. Burland
IBM
San Jose Research Center
5600 Cottle Road
San Jose, California 95143

Dr. John Cooper
Code 6130
Naval Research Laboratory
Washington, D.C. 20375

Dr. W. M. Jackson
Department of Chemistry
Howard University
Washington, D.C. 20059

Dr. George E. Walrafen
Department of Chemistry
Howard University
Washington, D.C. 20059

Dr. Joe Brandelik
AFWAL/AADO-1
Wright Patterson AFB
Fairborn, Ohio 45433

Dr. Carmen Ortiz
Cousejo Superior de
Investigaciones Cientificas
Serrano 117
Madrid 6, SPAIN

Dr. John J. Wright
Physics Department
University of New Hampshire
Durham, New Hampshire 03824

FILM

4-84